ISBN: 978-3-95450-214-1 ISSN: 2673-5490 doi:10.18429/JACoW-IPAC2021-THPAB200

CAVITY CONTROL MODELLING FOR SPS-TO-LHC BEAM TRANSFER STUDIES*

L. Medina†, T. Argyropoulos, P. Baudrenghien, H. Timko, CERN, Geneva, Switzerland

Abstract

To accurately simulate injection losses in the LHC and the High-Luminosity LHC era, a realistic beam distribution model at SPS extraction is needed. To achieve this, the beam-loading compensation by the SPS cavity controller has to be included, as it modulates the bunch positions with respect to the rf buckets. This dynamic cavity control model also allows generating a more realistic beam halo, from which the LHC injection losses will mainly originate. In this paper, the implementation of the present SPS cavity controller in CERN's Beam Longitudinal Dynamics particle tracking code is described. Just like in the machine, the feedback and feedforward controls are included in the simulation model, as well as the generator-beam-cavity interaction. Benchmarking against measurements of the generated beam distributions at SPS extraction are presented.

INTRODUCTION

During the first two operational periods of the LHC (Run 1 and Run 2), the SPS was operated with two 4-section and two 5-section travelling wave cavities (TWCs) [1, 2]. From 2021 onwards, two 4-section and four 3-section TWCs will be used to deliver beams for Run 3 and the High-Luminosity LHC (HL-LHC) [3–5]. To reduce the effective cavity impedance seen by the beam, a cavity controller using feedback (FB) and feedforward (FF) pathways is used for each cavity [6]. Detailed modelling of this system in particle tracking simulations is necessary to generate realistic beam distributions at SPS extraction, in particular, its bunch-by-bunch phase offsets with respect to the rf buckets and its halo population. These beams are used in SPS-to-LHC bunch-to-bucket transfer simulations [7, 8], where losses due to reduced LHC injection voltage are assessed. The study of a reduced injection voltage is conducted as a means to mitigate possible LHC power limitations in the HL-LHC era [9].

The model of the SPS cavity controller [10] has been implemented in CERN's Beam Longitudinal Dynamics (BLonD) [11–13] particle tracking suite; it contains models for the low-level rf (LLRF) module, its different filters, and the generator-beam-cavity interactions. Described step-by-step in the following, it also provides a guideline for the development of similar cavity control systems in beam simulation codes, as special considerations that need to be taken during the turn-by-turn (tbt) signal analysis are highlighted.

SPS CAVITY CONTROL

A simplified diagram of the one-turn delay FB system (OTFB) of the SPS LLRF implemented in BLonD is shown in Fig. 1. For simplicity, a single OTFB system is assigned to the group of n_{cav} equal TWCs with the same amount of sections. The total rf voltage seen by the beam is the sum of the cavity (*antenna*) voltage[1] $\vec{V}_{\mathrm{ant}}^{(m)}$ regulated by the OTFB for each cavity group $m = 1, 2$,

$$\vec{V}_{\mathrm{ant}} = \vec{V}_{\mathrm{ant}}^{(1)} + \vec{V}_{\mathrm{ant}}^{(2)} , \tag{1}$$

where

$$\vec{V}_{\mathrm{ant}}^{(m)}(t) = \vec{V}_{\mathrm{b}}^{(m)}(t) + \vec{V}_{\mathrm{g}}^{(m)}(t) , \tag{2}$$

that is, the sum of the beam- $\vec{V}_{\mathrm{b}}^{(m)}$ and generator- $\vec{V}_{\mathrm{g}}^{(m)}$ induced voltages. These signals span one turn, $t \in [0, T_{\mathrm{rev}}]$, with T_{rev} being the revolution period. Figure 2 shows the main signals in the cavity controller of a given cavity group, with $\vec{V}_{\mathrm{ant}}$ displayed at the bottom. The design (*set point*) rf voltage $\vec{V}_{\mathrm{set}}$ is partitioned ($p \in [0, 1]$) between the two TWC groups as $\vec{V}_{\mathrm{set}}^{(1)} = p\vec{V}_{\mathrm{set}}$ and $\vec{V}_{\mathrm{set}}^{(2)} = (1-p)\vec{V}_{\mathrm{set}}$. In the following, the super-index (m) is dropped for simplicity and all quantities correspond to the OTFB of a given partition unless stated otherwise. Depending on their nature, the different signals in the cavity controller are discretised with different samplings.

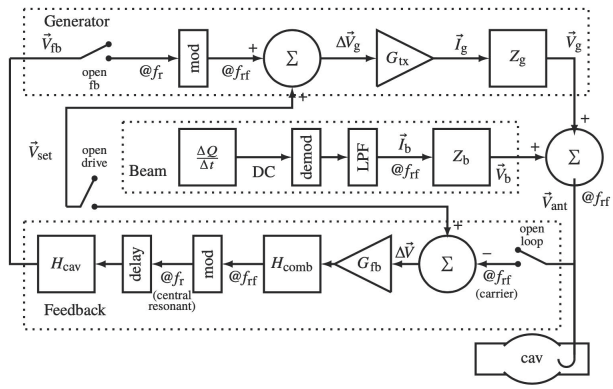

Figure 1: SPS cavity controller in BLonD. The correction to the rf voltage along each turn is calculated from the difference of the cavity (antenna) voltage (the sum of the beam and generator contributions), and the design (set-point) voltage.

One-Turn Delay Feedback

Each OTFB calculates the necessary correction to the cavity voltage to compensate beam-loading [14] and to regulate it to the design voltage $\vec{V}_{\mathrm{set}}$ of the corresponding partition, typically constant over a turn as shown in Fig. 2a. To compute it, the OTFB system first measures the difference between the antenna voltage $\vec{V}_{\mathrm{ant}}$ and the required set point

* Research supported by the HL-LHC project.
† lmedinam@cern.ch

[1] In complex notation, $\vec{X} = I + iQ = \mathrm{Re}(\vec{X}) + i\mathrm{Im}(\vec{X})$ for any signal $\vec{X}$.

ISBN: 978-3-95450-214-1 ISSN: 2673-5490 doi:10.18429/JACoW-IPAC2021-THPAB200

voltage,

$$\Delta\vec{V}_{(j)} = \vec{V}_{\mathrm{set},(j)} - \vec{V}_{\mathrm{ant},(j)}\,, \tag{3}$$

see Fig. 2b. The OTFB signals are sampled at the rf (carrier) frequency f_{rf} (j is the sample index), so the sampling time T_s is equal to the single-rf bucket length without intensity effects. The error signal is then processed with a comb filter (with scaling factor of $\alpha = 15/16$ and FB loop gain of G_{fb}) which compares it with the corresponding signal from the *previous* turn, effectively removing the beam-loading effect. Since the TWCs have a filling time τ, a complementary delay $T_{\mathrm{rev}} - \tau$ is then applied to make the total loop delay exactly one turn, with the result observed in Fig. 2c. The signal is then modulated to the TWCs' central resonance frequency $f_{\mathrm{r}} = 200.1$ MHz (measured), keeping its tbt continuity (accumulated phase offset must be taken into account). Once at f_{r}, the cavity response H_{cav}, modelled as a moving average sampled at 40 MS/s (corresponding to the typical bunch spacing), is applied to the signal, see Fig. 2d.

Generator-Induced Voltage

The correction computed by the FB system is used to regulate the generator drive. The generator current, discretised at the rf frequency, is given by the transmitter model,

$$\frac{\vec{Q}_{\mathrm{g}}}{T_s} = G_{\mathrm{tx}}\frac{\vec{V}_{\mathrm{set}} + \Delta\vec{V}_{\mathrm{fb}}}{R_{\mathrm{g}}}\,, \tag{4}$$

where $G_{\mathrm{tx}} \approx 1$ is the transmitter gain, $\Delta\vec{V}_{\mathrm{fb}}$ the OTFB correction demodulated back to the carrier frequency, and R_g the constant in the cavity impedance towards the generator (defined as $\rho L_{\mathrm{cav}}^2/8$, with ρ and L_{cav} the cavity series impedance and total cavity length, respectively) [1]. In Eq. (4), $\vec{Q}_{\mathrm{g}}$ is the instantaneous generator *charge* at each sample (Fig. 2f). Formally, charge signals are used for calculations in place of *current* signals in this discretised model. Note also that $\vec{Q}_{\mathrm{g}}$ is the total current in the generators of the TWC group. The generator-induced voltage $\vec{V}_{\mathrm{g}}$, Fig. 2g, is the result of the matrix convolution of the generator current with the impulse response matrix h_{g} from the cavity towards the generator,

$$\vec{V}_{\mathrm{b}} = h_{\mathrm{g}} * \vec{Q}_{\mathrm{g}}\,. \tag{5}$$

As the model acts on a tbt basis, continuity of the $\vec{Q}_{\mathrm{g}}$ signal must be ensured. The last samples of the previous turn are prepended to the present-turn data prior to the computation of $\vec{V}_{\mathrm{b}}$. From the convolution result, only the segment corresponding to the present turn is extracted. For beam tracking, $\vec{V}_{\mathrm{b}}$ is interpolated to the finer grid described below.

Beam-Induced Voltage

As in measurements, the beam profile λ is discretised at the bin positions $t_{(i)}$ of sample (i) with a resolution in the order of $O(2\text{–}3)$ S/bucket. The rf component at the angular carrier (rf) frequency of the beam charge is computed as

$$\vec{Q}_{\mathrm{b},(i)} = 2e\lambda(t_{(i)})\left[\cos(\omega_{\mathrm{rf}}t_{(i)}) + i\sin(\omega_{\mathrm{rf}}t_{(i)})\right]\,, \tag{6}$$

and shown in Fig. 2h. Similarly to the generator, the total beam-induced voltage $\vec{V}_{\mathrm{b}}$ in the n_{cav} TWCs of the partition

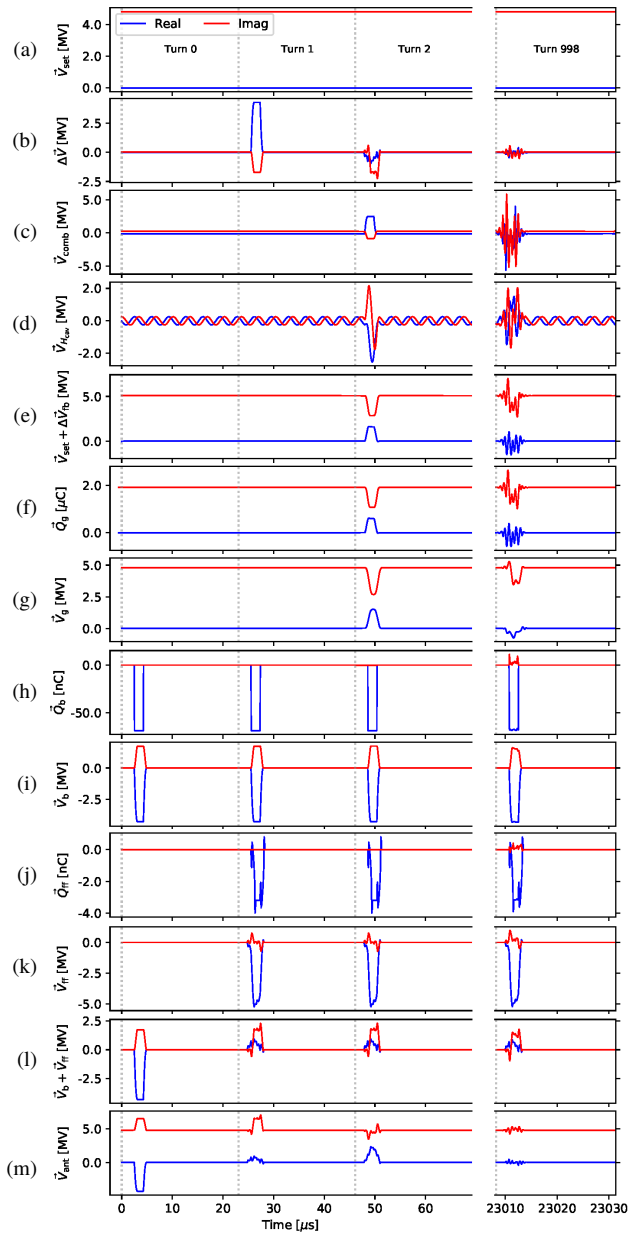

Figure 2: Main signals in the BLonD SPS cavity controller model of the two 4-section TWCs (voltage partitioning of 0.4828 × 10 MV, single rf). Test with 72 bunches (2.3×10^{11} protons/bunch, 1.20 ns bunch length), $G_{\mathrm{fb}} = 10$, and $G_{\mathrm{ff}} = 1$. Tracking for 1×10^3 turns at flat-top with the first three and last turns plotted. At the first turn, $\vec{V}_{\mathrm{ant}}$ is disturbed from $\vec{V}_{\mathrm{set}}$ by beam-loading; from the second turn onwards, the FF and FB (slower) corrections are visible; at the last turn, a good correction of $\vec{V}_{\mathrm{ant}}$ in the beam segment is achieved.

(Fig. 2i) is the result of convolving the beam impulse response h_{b} with the rf beam current,

$$\vec{V}_{\mathrm{b}} = h_{\mathrm{b}} * (n_{\mathrm{cav}}\vec{Q}_{\mathrm{b}})\,. \tag{7}$$

The beam-induced voltage, computed at each turn at the finer profile bin positions, is downsampled to the (j)-grid

ISBN: 978-3-95450-214-1 ISSN: 2673-5490 doi:10.18429/JACoW-IPAC2021-THPAB200

for the OTFB calculations. The circularity of the $\vec{Q}_\mathrm{b}$ signal is relevant when the beam spans a full turn.

Feedforward

The performance of the FB correction can be further increased by adding the FF loop. Implemented as a finite-impulse response (FIR) filter [15] with n_ff taps, the correction by the FF to the total induced voltage at a given turn is computed based on the beam current from the previous turn. With the feedforward signals being sampled at the bunch separation T_bb (every five buckets, or about 25 ns),

$$\vec{Q}_{\mathrm{ff},(k)} = \sum_{l=0}^{n_\mathrm{ff}} c_l \vec{Q}_{\mathrm{b,prev},(k-l)} \,, \tag{8}$$

see Fig. 2j, where (k) is the sample index and c_l the n_ff normalised coefficients of the FIR filter, specific for each cavity type. When considering the filter delay of $\frac{1}{2}(n_\mathrm{ff}-1)T_\mathrm{bb}$ and the cavity filling time in the loop, the present-turn $\vec{Q}_\mathrm{b}$ signal must then be appended to $\vec{Q}_\mathrm{b,prev}$, as the FF correction starts by the end of the previous turn. The corresponding voltage to Eq. (8) is calculated similarly to Eq. (5),

$$\vec{V}_\mathrm{ff} = G'_\mathrm{ff}\, h_\mathrm{g} * (n_\mathrm{cav}\vec{Q}_\mathrm{ff}) \,, \tag{9}$$

where h_g is downsampled to (k) and G'_ff is the FF gain G_ff scaled by $R_\mathrm{b}/R_\mathrm{g}$ (where $R_\mathrm{b} \equiv L_\mathrm{cav}\sqrt{\rho Z_0/2}$ the constant in the cavity impedance towards the beam [1] and $Z_0 = 50\,\Omega$ the measured shunt impedance). The present-turn $\vec{V}_\mathrm{ff}$ correction, Fig. 2k, is extracted considering the filter delay and linearly interpolated to the higher-resolution generator and beam signals; then, it is added to the beam component of the total voltage with a negative sign for compensation (Fig. 2l),

$$\vec{V}'_\mathrm{b} = \vec{V}_\mathrm{b} - \vec{V}_\mathrm{ff} \,. \tag{10}$$

Other Considerations

Beam-loading is reduced on a tbt basis by the FB and FF loops and the total voltage $\vec{V}_\mathrm{ant}$ is regulated to the design voltage $\vec{V}_\mathrm{set}$ with a precision depending on the FB gain. The controller needs to be switched on and tracked without beam first, to allow for the voltages to reach steady state without beam. For particle tracking, the design rf voltage seen by the beam, by default constant in amplitude V_rf and phase ϕ_rf over a turn in BLonD, is replaced at the profile resolution by

$$V_{\mathrm{rf},(i)} = V_\mathrm{rf}\frac{V_{\mathrm{ant},(i)}}{V_\mathrm{rf}} \sin\left(\omega_\mathrm{rf} t_{(i)} - \phi_\mathrm{rf} + \Delta\varphi_{\mathrm{ant},(i)}\right) \,, \tag{11}$$

where V_ant and $\Delta\varphi_\mathrm{ant}$ are the amplitude and phase of the total antenna voltage, i.e. the sum of the two partitioned voltages regulated by their respective OTFB systems (Eq. (1)). For multi-harmonic rf systems, the contribution from additional rf harmonics should be added to the equation above.

BENCHMARK AND CALIBRATION

The measured bunch-by-bunch position offsets $\Delta\phi_\mathrm{bb}$ of a 72-bunch batch with nominal intensity are shown in Fig. 3; they are compared with the expected result using a static impedance-reduction model for beam-loading compensation

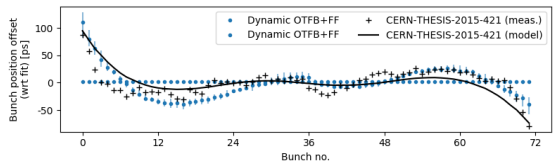

Figure 3: Bunch position offsets of a 72b batch generated at SPS flat-top with OTFB and comparison with static model.

used in previous simulations [16]. Using the same beam parameters, tracking at SPS flat-top with the present cavity controller shows the results to be in better agreement with measurements. Generated beam distributions with the dynamic OTFB have the added advantage of a more realistically described beam halo, crucial for LHC injection loss studies. Calibration of the OTFB parameters (transmitter, FB, and FF gains) was conducted to reproduce the measurements of several batches from Run 2 (2018) fills; results for $\Delta\phi_\mathrm{bb}$ match well beam measurements, with full details given in [8]. The SPS 800 MHz rf system is added to the total rf voltage with a fixed phase offset of 180 degrees w.r.t. to the main 200 MHz system, but no cavity control is included. The benchmark of realistic HL-LHC beams requires power clamping at 1.0 MW and 1.6 MW for the 3-section and 4-section TWCs, respectively, a currently ongoing work [17, 18]. The possibility of clamping the generator current at a given power threshold has been implemented to simulate these power limitations [2]. With the actual physical generator current given by $\vec{I}_\mathrm{g} = (\vec{Q}_\mathrm{g}/n_\mathrm{cav})/T_\mathrm{bb}$, the generator power per cavity is found as $P_g = \frac{1}{2}Z_0|\vec{I}_\mathrm{g}|^2$.

The computation of the matrix convolutions in Eqs. (5) and (7) is run-time heavy due to the long duration of the signals involved. In the code, it is implemented using Scipy's `fttconvolve` function [19], which uses FFT for performance. This can lead, however, to edge effects on the tbt signals (independently of the chosen boundary conditions) which could then be enhanced by the feedback loops.

CONCLUSION

Mirroring the system in the real machine, the implementation of the SPS cavity controller and its different filters has been done in BLonD. Beam generation at SPS flat-top with realistic $\Delta\phi_\mathrm{bb}$ and halo dynamics can be achieved using the present cavity controller model, with the resulting distributions being used in studies of LHC and HL-LHC injection losses. As the bucket-by-bucket correction to the rf voltage is calculated on a tbt basis by the one-turn delay feedback, special care was taken to ensure that the different current and voltage signals in the low-level rf, generator, and beam models are continuous and computationally accurate. Work on coupling the cavity feedback with global feedback systems, such as the SPS beam phase loop, is ongoing.

ACKNOWLEDGEMENTS

The authors thank H. Damerau, G. Hagmann, W. Höfle, T. Mastoridis, and E. Shaposhnikova and for fruitful discussions and comments.

ISBN: 978-3-95450-214-1 ISSN: 2673-5490 doi:10.18429/JACoW-IPAC2021-THPAB200

REFERENCES

[1] G. Dôme, "The SPS acceleration system travelling wave drift-tube structure for the CERN SPS," CERN, Geneva, Switzerland, Rep. CERN-SPS-ARF-77-11, May 1977.

[2] T. Bohl, "Running RF with high beam loading. The 200 MHz travelling wave cavities in the SPS," in *Proc. 10th Workshop on LEP-SPS Performance*, Chamonix, France, Jan. 2000, pp. 56–60.

[3] The High Luminosity LHC Project, https://hilumilhc.web.cern.ch

[4] H. Damerau *et al.*, "LIU: exploring alternative ideas," in *Proc. of RLIUP: Review of LHC and Injector Upgrade Plans*, Archamps, France, Oct. 2013, pp. 127–137. doi:10.5170/CERN-2014-006.127

[5] G. Hagmann *et al.*, "The CERN SPS Low Level RF upgrade Project," in *Proc. 10th Int. Particle Accelerator Conf. (IPAC'19)*, Melbourne, Australia, Jun. 2019, pp. 4005–4008. doi:10.18429/JACoW-IPAC2019-THPRB082

[6] P. Baudrenghien and G. A. Lambert, "Reducing the impedance of the travelling wave cavities: feed-forward and one turn delay feed-back," in *Proc. 10th Workshop on LEP-SPS Performance*, Chamonix, France, Jan. 2000, pp. 94–101.

[7] H. Timko, T. Argyropoulos, I. Karpov, and E. Shaposhnikova, "Beam instabilities after injection to the LHC," in *Proc. 61st ICFA Advanced Beam Dynamics Workshop (HB'18)*, Daejeon, Korea, Jul. 2018, pp. 163–167. doi:10.18429/JACoW-HB2018-TUP1WA03

[8] L. E. Medina Medrano, T. Argyropoulos, R. Calaga, and H. Timko, "Studies of Longitudinal Beam Losses at LHC Injection", presented at the 12th Int. Particle Accelerator Conf. (IPAC'21), Campinas, Brazil, May 2021, paper THPAB199.

[9] L. Medina *et al.*, "LHC MD 3165: RF power limitations at flat bottom," CERN, Geneva, Switzerland, Rep. CERN-ACC-NOTE-2019-0030, Jul. 2019.

[10] D. Boussard, "Control of cavities with high beam loading," *IEEE Transactions on Nuclear Science*, vol. 32, no. 5, pp. 1852–1856, Oct. 1985. doi:10.1109/TNS.1985.4333745

[11] CERN BLonD Simulation Suite website, http://blond.web.cern.ch

[12] CERN BLonD Simulation Suite code repository, https://github.com/blond-admin/BLonD

[13] H. Timko *et al.*, "Beam Longitudinal Dynamics Simulation Suite BLonD," to be published.

[14] D. Boussard, "Beam loading (particle accelerators)," in *Proc. CAS - CERN Accelerator School: 5th Advanced Accelerator Physics Course*, Rhodes, Greece, 1995, pp. 415–436. doi:10.5170/CERN-1995-006.415

[15] P. Baudrenghien and T. Mastoridis, "I/Q model of the SPS 200 MHz Travelling Wave Cavity and feedforward design," CERN, Geneva, Switzerland, Rep. CERN-ACC-NOTE-2020-0032, May 2020.

[16] T. Argyropoulos, "Longitudinal beam instabilities in a double RF system," Ph.D. thesis, Phys. Dept., Natl. Tech. University, Athens, Greece, Jan. 2015.

[17] I. Karpov, H. Damerau, G. Papotti, E. Shaposhnikova, T. Mastoridis, and P. Baudrenghien, "Update on RF power requirements," presented at the LIU-SPS Coordination Meeting, CERN, Geneva, Switzerland, Aug. 2020, unpublished.

[18] T. Mastoridis and P. Baudrenghien, "TWC 200 field regulation at SPS extraction, HL-LHC beam", CERN, Geneva, Switzerland, Aug. 2020, private communication.

[19] SciPy Reference Guide, https://docs.scipy.org/doc/scipy/reference/generated/scipy.signal.fftconvolve.html